

# Does PAMELA $\bar{p}/p$ measurements affect the prospects of dark matter indirect detection at LHC?

Céline Boehm,<sup>1</sup> Timur Delahaye,<sup>1,2</sup> Pierre Salati,<sup>1</sup> Florian Staub,<sup>3</sup> and Ritesh K. Singh<sup>3</sup>

<sup>1</sup>LAPTH, Université de Savoie, CNRS, BP110, F-74941 Annecy-le-Vieux Cedex, France\*

<sup>2</sup>Dipartimento di Fisica Teorica, Università di Torino and INFN Sezione Torino, via P. Giuria 1, I10125 Torino, Italy<sup>†</sup>

<sup>3</sup>Institut für Theoretische Physik und Astronomie, Universität Würzburg, 97074 Würzburg, Germany<sup>‡</sup>

(Dated: today)

Since the PAMELA results on the “anomalously” high positron fraction and the lack of antiproton excess in our Galaxy, there has been a tremendous number of studies advocating new types of dark matter, with larger couplings to electrons than to quarks. Is this feature a bad sign for the dark matter detection prospects at LHC? Since the WIMP couplings to quarks are constrained by PAMELA, the question of the production of dark matter (and heavy associated coloured states) at LHC definitely arises. Here we show that, despite the agreement between the PAMELA antiproton measurements and the expected astrophysical secondary background, the WIMP couplings to heavy quarks can actually be larger than the strong coupling constant. Thus PAMELA  $\bar{p}/p$  measurements are not really challenging dark matter models. In addition, large values of the WIMP coupling to quarks suggest that heavy coloured states might be produced significantly in quark-quark collisions. We therefore investigate if this is an interesting channel to study at LHC. Finally, our analysis delineates the region of parameter space which both saturates the limits from PAMELA  $\bar{p}/p$  measurements and jeopardizes the conventional scenario for WIMP thermal decoupling in the early universe.

## I. INTRODUCTION

The new results of experiments such as PAMELA [1, 2], ATIC [3], HESS [4], FERMI [5] have attracted a lot of attention in the dark matter community during the last few months [6, 7, 8, 9] and somehow revived hopes that cosmic ray data could finally shed light on the nature of dark matter. In particular, the apparent conflict between the seemingly excess in the positron fraction and the lack of visible anomalies in the antiproton spectrum has encouraged theoreticians to propose new dark matter models with very unusual properties. For example, to fit PAMELA data, a large amount of dark matter models with very large values of the annihilation cross section into leptons and small values of the annihilation cross section into quarks have been proposed in the literature. All these models rely on “local” enhancement mechanisms so that the candidate abundance remains compatible with the measured dark matter relic density while, simultaneously, leading to a high amount of positrons in our galaxy. This illustrates the complexity of the mechanisms invoked and reflects the ongoing theoretical effort to explain the PAMELA positron excess. Alternatively, this positron anomaly could be the signature of nearby pulsars supplementing the interstellar medium with a radiation of electrons and positrons. The possibility that spallation reactions take place during the acceleration of primary cosmic rays has finally been suggested.

In this article, we concentrate on the antiproton measurements which are subject to neither speculation nor controversial interpretation. It has been shown indeed that the PAMELA antiproton to proton ratio turns out to be compatible with a pure astrophysical explanation. Antiprotons are generated inside the galactic disc and result from the interaction of high en-

ergy cosmic ray protons and helium nuclei on the interstellar material. The lack of excess in antiprotons indicates that the WIMP couplings to quarks must be small. How small these couplings are is a crucial problem with respect to the detection of dark matter species at the LHC.

To answer this question, we base our analysis on a generic dark matter model where the WIMP  $\chi$  is directly coupled to a standard model quark  $q$  and a heavy coloured partner  $F_q$ . Inspired by supersymmetry, we shall focus this Letter on a Majorana WIMP so  $F_q$  is in fact a scalar (and would be equivalent to squarks). Our approach is generic enough to be applied to other types of dark matter. However a complete survey of the various possibilities (including scalar dark matter species  $\chi$  and fermionic partner  $F_q$ ) is beyond the scope of this work (although we anticipate that the results presented here are fairly general).

In proton-proton collisions, the heavy states  $F_q$  can be produced through  $qq$ ,  $q\bar{q}$ ,  $qg$  and  $gg$  interactions. The three former types of production directly involve the coupling to dark matter while the latter involves the strong coupling constant. Once produced, the heavy coloured states  $F_q$  are expected to decay into missing energy (the dark matter) and a jet (corresponding to the quark  $q$ ), hence the importance of the strength of the WIMP couplings to quarks and antiquarks in both type of  $F_q$  production. In this letter, we investigate how the lack of antiproton excess reported by PAMELA constrains the WIMP coupling to quarks and the dark matter and  $F_q$  masses. We investigate also the production of heavy states (and subsequently of WIMPs) at LHC due to quark quark collisions. In particular, we determine whether this production is significant in spite of the limits set by PAMELA on the WIMP coupling to quarks and anti quarks or whether it is suppressed with respect to the gluon fusion production  $gg \rightarrow F_q\bar{F}_q$ .

To constrain the dark matter characteristics (mass and properties of the particles to which dark matter is coupled), we proceed as follows: we first use a realistic cosmic ray propagation code to calculate the antiproton flux at the earth expected from conventional spallations and dark matter annihilations. The

\*Electronic address: celine.boehm@cern.ch

<sup>†</sup>Electronic address: timur.delahaye@lapp.in2p3.fr

<sup>‡</sup>Electronic address: florian.staub@physik.uni-wuerzburg.de

latter depend on the  $\chi - q - F_q$  left and right couplings  $c_L^q$  and  $c_R^q$  which we want to constrain from the PAMELA antiproton measurements. We then consider in Sec. II a variety of annihilation channels and derive the maximal cross sections allowed by the PAMELA antiproton data. Results are expressed in units of the canonical thermal value of  $3 \times 10^{-26} \text{ cm}^3 \text{ s}^{-1}$  and referred to as the boost factor hereafter. Because couplings to  $u$ ,  $d$  and  $s$  quarks are already severely constrained by direct detection, we focus on  $c$  and  $b$  quarks. With the help of a Monte Carlo Markov chain, we delineate in Sec. III the region of parameter space which saturates the upper bound on the boost. Finally, in Sec. IV, we determine the number of events associated with  $qq \rightarrow FF$ ,  $q\bar{q} \rightarrow FF^*$  and  $qg \rightarrow F\chi$  production at LHC and discuss the prospects for detecting dark matter related signatures at LHC. We conclude in Sec. V.

## II. THE PAMELA ANTIPROTON CONSTRAINTS

The antiproton flux at the earth arises from two sources. Conventional (secondary) antiprotons are produced by the interactions of high energy cosmic ray protons and helium nuclei with the gas of the galactic disc. The annihilation of hypothetical dark matter species in the halo of the Milky Way generates additional (primary) antiprotons. To compute both signals, we have considered the same propagation model as in [10] with the parameters best fitting the boron to carbon ratio [11]. As regards the secondary component, we have used the same local proton and helium nuclei fluxes as in [12] together with the radial distribution of SN remnants given by [13] to retro-propagate these fluxes all over the diffusive halo.

Concerning the primaries, we have considered a dark matter halo computed by [14] with a local density of  $\rho_\odot = 0.3 \text{ GeV cm}^{-3}$ . The distance from the earth to the galactic center is 8.5 kpc. The annihilation cross section is set to the conventional thermal value mentioned above. We have determined the boost by which that value can be increased without exceeding the PAMELA data. We have scanned the WIMP mass from 100 GeV to 1 TeV and considered different annihilation channels. For each channel, the antiproton spectrum before propagation has been calculated with the PYTHIA 6.4 program [15]. The results are summed up in Tab. I.

These constraints are quite severe. However, antiproton flux calculations suffer from a lot of uncertainties and changing some of the choices we made may affect these results. As recalled in [16] the local value of the dark matter density is not very well constrained and in fact lies in  $[0.2; 0.9] \text{ GeV cm}^{-3}$ . The primary antiproton flux being proportional to the square of the local density, one can multiply all the results of Tab. I by a factor ranging from  $\sim 0.4$  to 9. The other uncertainties are summed up in Tab. II.

One should notice that for most cases, the constraints come from the point of highest energy (61.2 GeV) published by PAMELA. This point is the one that suffers the biggest statistical error and its systematic error is unknown yet. Hence the results may change with future publication of new PAMELA data. Indeed the current data correspond to only 500 days of data collection starting the 15th of June 2006 but the satel-

	u $\bar{u}$	d $\bar{d}$	s $\bar{s}$	c $\bar{c}$	b $\bar{b}$	g g	h h	Z <sub>0</sub> Z <sub>0</sub>	w <sup>+</sup> w <sup>-</sup>
100	2	2	2	2	3	2			
200	4	3	3	5	6	3		6	6
300	5	4	4	5	9	5	9	9	7
400	6	5	5	6	10	6	14	9	8
500	7	6	7	8	11	7	14	11	9
600	8	8	8	9	12	7	15	12	11
700	10	9	10	11	13	8	16	14	13
800	12	11	11	12	15	9	17	16	16
900	14	13	13	14	17	10	19	19	18
1000	16	15	15	16	19	11	21	22	21

TABLE I: Maximum annihilation cross section allowed by the PAMELA antiproton measurements for various WIMP masses and different annihilation channels. This cross section is expressed in units of the canonical value of  $3 \times 10^{-26} \text{ cm}^3 \text{ s}^{-1}$ .

	ref	1	2	3	4	5	6	7
100	3	28	2	4	4	6	2	2
200	6	60	3	8	6	11	3	4
300	9	90	4	13	10	18	5	5
400	10	130	4	15	11	22	7	6
500	11	150	4	16	12	23	9	6
600	12	170	4	18	13	26	10	7
700	13	190	5	20	15	29	11	8
800	15	220	6	23	17	33	12	9
900	17	240	6	26	19	38	14	10
1000	19	270	7	29	21	42	16	11

TABLE II: Maximum boost allowed by the PAMELA antiproton measurements for various WIMP masses in the case of annihilation into  $b\bar{b}$  pairs when varying the parameters. Cases 1 and 2 correspond to extreme propagation parameters in agreement with B/C. For case 2 the boost has been rounded to the closest decade. Cases 3, 4 and 5 correspond to various dark matter halo profiles : NFW [17] (3), Moore [18] (4) and an isothermal cored profile (5). Cases 6 and 7 correspond to alternative fits of the injection proton and helium nuclei spectra respectively proposed by [10] and [19].

lite is still in orbit and should carry on taking data for at least few more months. Moreover, the uncertainty related to the injection spectra should diminish as soon as absolute fluxes for protons and antiprotons are published. Finally, new data are also expected from PAMELA for the boron to carbon ratio that should help us limit the uncertainties on propagation parameters.

## III. THE MCMC AND THE ALLOWED REGION IN PARAMETER SPACE

To find the region of the parameter space which reproduces the boost factor as determined in the previous section, we perform Markov Chain Monte Carlo simulations. The free parameters in our model are the dark matter mass, the masses of the exchanged particles, and their couplings to Standard Model particles. Since  $b$ -quarks are a bit easier to tag, we shall focus

only on predictions associated with  $b$  quarks. The only free parameters of interest are therefore the mass of the  $b$ -coloured states  $m_{F_b}$ , the dark matter mass  $m_\chi$  and its couplings to  $b$  quarks, namely  $c_L^b$  and  $c_R^b$ . In total, we have four free parameters ( $m_\chi, m_{F_b}, c_L^b, c_R^b$ ) that we shall determine by comparing the value of the annihilation cross section, found for a particular set of parameters, with the value of the boost found in Sec. II. The expression of the annihilation cross section that we consider is taken from [20]. The range of masses and couplings that we consider lies between [100, 2500] GeV and [0.001, 3] respectively. One could, in fact, consider a larger upper limit for the couplings but one may lose perturbativity.

To perform the simulation, we use a Gaussian proposal distribution function, centred on the origin:

$$Q = e^{-\left(\frac{\varepsilon_i^2}{2\sigma_i^2}\right)},$$

where  $\sigma_i$  is the variance in the dimension  $i$  and  $\varepsilon_i$  the displacement in the  $i$ -th dimension that brings the chain from point  $x_i^{(t)}$  at step  $t$  to point  $x_i^{(t+1)}$  at step  $t+1$ . Since  $\varepsilon_i$  is sampled from a symmetric proposal distribution function, we can apply the Metropolis-Hatkins algorithm, that is:

when the likelihood distribution function ( $\mathcal{L}_2$ ) of the new point  $x_i^{t+1}$  is larger than the likelihood  $\mathcal{L}_1$  of the previous point  $x_i^{(t)}$ , the point  $x_i^{(t+1)}$  is accepted and appended onto the chain which then moves to  $x_i^{(t+1)}$ . If  $\mathcal{L}_2 < \mathcal{L}_1$ , one randomly samples a probability  $p$  by using a flat uniform distribution. If the ratio  $\mathcal{L}_2/\mathcal{L}_1$  is greater than  $p$ , the point  $x_i^{t+1}$  is appended onto the chain. Otherwise, the point is rejected and the chain stays at the same position (that is  $x_i^t$ ) until a point with better likelihood is found.

In the above description, we have actually assumed flat priors for the four parameters. Hence the probability that a set of parameters corresponding to model X is favoured given the data over another set of parameters corresponding to model Y is actually equivalent to the ratio of the likelihood of the two models, that is.:

$$\frac{p(Y|data)}{p(X|data)} = \frac{\mathcal{L}_Y}{\mathcal{L}_X}.$$

To scan the entire parameter space, we use relatively large values of the variance  $\sigma_i$ . To avoid seeing the effect of the seeds of the generator, we first run a chain with unlimited number of points. The sole requirement that we apply on this chain is to find a point with relatively good likelihood value. Once such a point is found, we burn-in the chain by setting the last point of this chain as the starting point of a new chain and then run a chain of 300000 points. In total, we have run ten chains of 300,000 points.

Results are displayed in the correlation plots of Fig. 3. The first four rows correspond to the parameters  $m_\chi$ ,  $m_{F_b}$ ,  $c_L^b$  and  $c_R^b$  of the model while the last one is the MC prediction for the Boost factor, as defined in section II.

The panel in the very first line represents the dark matter mass while the last panel of the second, third and fourth rows stands

for  $m_{F_b}$ ,  $c_L^b$  and  $c_R^b$  respectively. The first panel of the second line is a correlation plot between  $m_{F_b}$  and  $m_\chi$ . The first (second) plot in the third line features the correlation between  $c_L^b$  and  $m_\chi$  ( $c_L^b$  and  $m_{F_b}$ ) and so on.

The dotted lines in all the plots feature the prior distribution while the solid line is the posterior distribution (the values of the parameters that are favoured by the Markov chain).

The chain has explored enough points since the prior distributions are indeed rather flat for the four parameters and matches a Gaussian distribution for the boost.

We can also check that the constraint of dark matter stability ( $m_{F_b} > m_{dm}$ ) is correctly reproduced in the  $m_{F_b}, m_\chi$  plot of the second row. Notice that the boost factor scales correctly with dark matter mass.

If we assume that the boost factor, as determined in Sec. II, is an exact value (for example  $B = B_{found} \pm 0.01$ ), we find that the preferred values of  $m_{F_b}$  and the couplings are rather large. In this case, indeed, both left and right handed couplings can reach two or three units (with 95% and 68% CL respectively). If we consider a larger variance ( $B = B_{found} \pm \nu_B$  with  $\nu_B$  large), we observe a larger correlation between these two couplings. Although slightly smaller values of the boost  $B$  can be in principle achieved with simultaneously large values of the couplings and mass  $m_{F_b}$ ,  $m_{F_b}$  would have to be larger than the 2.5 TeV limit that we set. Hence, in this case, our Monte Carlo prefers a large value of one of the coupling (e.g.  $c_L^b$ ) together with a smaller value of the other coupling (e.g.  $c_R^b$ ) and a large value of  $m_{F_b}$  (still within our limits).

Note that the correlation plots displayed in Fig. 3 are obtained by saturating the upper limit on the boost obtained in section II. The parameters found in these plots therefore correspond to a large annihilation cross section into quarks, which translates into a relic density smaller than  $\Omega_{dm} h^2 = 0.1099 \pm 0.0062$  [21].

Since our model simply relies on WIMP couplings to quarks (we do not invoke the Sommerfeld mechanism for example), we thus have delineated the region of the parameter space where WIMPs have The region of parameter space which matches an acceptable thermal relic abundance is less promising for LHC than what is found here from the sole PAMELA antiproton measurements. Discovering heavy coloured states at LHC decaying into jet+missing energy and with properties matching this region of the parameter space would jeopardize conventional dark matter scenarios.

#### IV. HEAVY STATES PRODUCTION AT LHC

In spite of the PAMELA constraints, the WIMP couplings to quarks can be sufficiently large so that the question of  $F_q$  production at LHC from quark-quark collisions arises. We are interested in fact in  $bb \rightarrow F_b F_b$  (which may happen if dark matter is a real scalar or, in our case, a Majorana particle),  $b\bar{b} \rightarrow F_b \bar{F}_b$  and  $qg \rightarrow F_b \chi$ .

In Fig. 1,2, we display the values of these cross sections (expressed in fb) for the set of parameters chosen by our Monte Carlo. Interestingly enough, the  $qq \rightarrow FF$  and  $qg \rightarrow F\chi$  cross section cross sections can reach up a few pb and about three

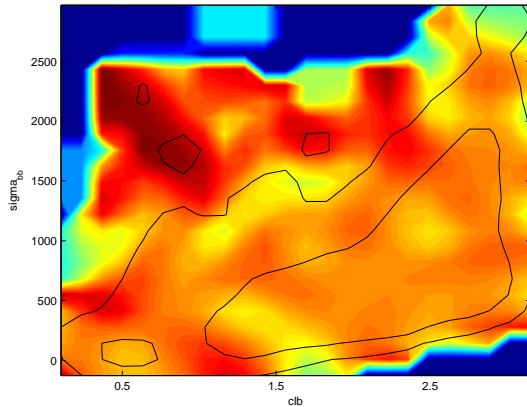


FIG. 1: The  $bb \rightarrow F_b F_b$  cross section vs the left-handed coupling to b quark, assuming negligible variance for  $\sqrt{s} = 14$  TeV. Results for  $\sqrt{s} = 10$  TeV (which is the centre of mass energy expected at the start of LHC) are quite similar.

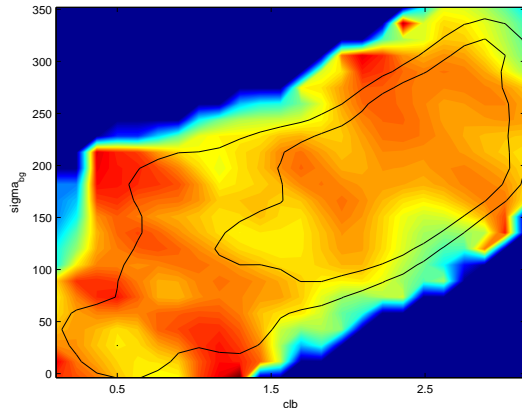


FIG. 2: The  $qg \rightarrow F\chi$  cross section versus the left handed coupling to b quark, assuming negligible variance for  $\sqrt{s} = 14$  TeV

hundred fb respectively for large couplings. Notice also the shape of the correlation between the  $bb \rightarrow F_b F_b$  and  $bg \rightarrow F_b \chi$  processes (see Fig.3).

Such large cross sections seem rather encouraging. However, to get realistic estimates, one has to take into account the parton distribution function (pdf) associated with b-quarks and gluons. By focusing on  $b$ , we have definitely considered a case where there is a very large suppression due to the pdf [22]. However, the pdf for  $c$  quarks is also suppressed and the boost factor is not so large. Hence  $b$  quarks are more or less representative of what is to be expected at LHC given of PAMELA antiproton measurements and the absence of WIMP couplings to  $u, d, s$  valence quarks, as indicated by direct detection.

At large  $x$  and  $Q^2$ , convoluting our cross section with the parton distribution function leads to a large suppression of the number of events. We predict much less than a few hundred events for  $bb \rightarrow F_b F_b$  in the region where the process is sup-

posed to be maximal (i.e. for large couplings). The  $qg \rightarrow F\chi$  cross section is less suppressed (still a few hundred fb) since it involves gluon. Both cases probably lead to a too small number of events (given that it would be a pure hadronic final state and we did not include the study of the kinematics) to be detected via the decay (jet+missing energy) of the heavy coloured states  $F_b$ .

## V. CONCLUSION

We have investigated the constraints that PAMELA set on the WIMP couplings to quarks and observed that coupling values larger than the strong coupling constant could be allowed by PAMELA antiproton measurements. This encouraged us to look at the production of heavy coloured final states from heavy quark collisions. We focus on b quarks in particular, since they might be easier to tag than c-quarks. Also we ignore couplings to  $u, d, s$  quarks since dark matter direct detection constraints indicate that these must be suppressed.

We find that, despite the large values of the cross sections (and the very large values of the WIMPs couplings to quarks), there is very little hope to produce a large number of coloured states  $F_b$  due to the b quark pdf suppression (less than a few 100 events at LHC for most of the parameter space under consideration). Also, such a final state would be purely hadronic and would be difficult to disentangle from background. Hence, the best channel to constrain the WIMP couplings to quarks may be, indeed, heavy coloured states production via gluon fusion and their decay into jets plus missing energy.

Although there have been many studies advocating leptophilic dark matter particles to fit the PAMELA positron excess, our analysis shows that the PAMELA antiproton measurement also allows for quarkphilic dark matter in principle. This property may hold whether dark matter is at the origin of the positron excess or not. To fit both PAMELA antiproton data and positron excess, it therefore seems likely that only the WIMP couplings to gauge boson may have to be suppressed. Large WIMPs couplings to heavy quarks may be difficult to constrain using LHC data since their effect on the cross section can be compensated by very large  $F_q$  masses. Not only would the LHC luminosity be too small to reach the region of interest but also, there would be a too small number of purely hadronic events produced in proton proton collisions. Hence, if supersymmetry or other well established models are not found at LHC, such a type of dark matter particles may be difficult to exclude using the specific channel under study in this paper.

### Acknowledgments

We are grateful to Peter Skands who was very kind to help us in dealing with Pythia code, J. Hamann and J. Lesgourgues for their help with getdist routine. We would like to thanks F. Arleo, F. Boudjema, J. Idarraga and W. Porod for fruitful

discussions. T.D. is grateful for financial support from the Rhône-Alpes region (Explora'Doc) and from the International Doctoral school in AstroParticle Physics (IDAPP). F.S. is supported by the DFG Graduiertenkolleg GRK-1147 while the work of R.K.S. is supported by the German BMBF under contract 05HT6WWA.

- 
- [1] O. Adriani, G. C. Barbarino, G. A. Bazilevskaia, R. Bellotti, M. Boezio, E. A. Bogomolov, L. Bonechi, M. Bongi, V. Bonvicini, S. Bottai, et al., *Nature (London)* **458**, 607 (2009), 0810.4995.
  - [2] O. Adriani, G. C. Barbarino, G. A. Bazilevskaia, R. Bellotti, M. Boezio, E. A. Bogomolov, L. Bonechi, M. Bongi, V. Bonvicini, S. Bottai, et al., *Physical Review Letters* **102**, 051101 (2009), 0810.4994.
  - [3] J. Chang, J. H. Adams, H. S. Ahn, G. L. Bashindzhagyan, M. Christl, O. Ganel, T. G. Guzik, J. Isbert, K. C. Kim, E. N. Kuznetsov, et al., *Nature (London)* **456**, 362 (2008).
  - [4] H. E. S. S. Collaboration: F. Aharonian, *ArXiv e-prints* (2009), 0905.0105.
  - [5] A. A. Abdo, M. Ackermann, M. Ajello, W. B. Atwood, M. Axelsson, L. Baldini, J. Ballet, G. Barbiellini, D. Bastieri, M. Batteino, et al., *Physical Review Letters* **102**, 181101 (2009), 0905.0025.
  - [6] L. Bergstrom, T. Bringmann, and J. Edsjo (2008), 0808.3725.
  - [7] D. Hooper, A. Stebbins, and K. M. Zurek (2008), 0812.3202.
  - [8] M. Lattanzi and J. I. Silk (2008), 0812.0360.
  - [9] M. Cirelli, M. Kadastik, M. Raidal, and A. Strumia, *Nuclear Physics B* **813**, 1 (2009), 0809.2409.
  - [10] F. Donato, D. Maurin, P. Salati, A. Barrau, G. Boudoul, and R. Taillet, *Astrophys. J.* **563**, 172 (2001), arXiv:astro-ph/0103150.
  - [11] D. Maurin, F. Donato, R. Taillet, and P. Salati, *Astrophys. J.* **555**, 585 (2001).
  - [12] F. Donato, D. Maurin, P. Brun, T. Delahaye, and P. Salati, *Phys. Rev. Lett.* **102**, 071301 (2009), 0810.5292.
  - [13] W. R. Webber, M. A. Lee, and M. Gupta, *Astrophys. J.* **390**, 96 (1992).
  - [14] J. Diemand et al. (2008), 0805.1244.
  - [15] T. Sjostrand, S. Mrenna, and P. Skands, *JHEP* **05**, 026 (2006), hep-ph/0603175.
  - [16] G. Jungman, M. Kamionkowski, and K. Griest, *Physics Reports* **267**, 195 (1996), arXiv:hep-ph/9506380.
  - [17] J. F. Navarro, C. S. Frenk, and S. D. M. White, *Astrophys. J.* **490**, 493 (1997), astro-ph/9611107.
  - [18] J. Diemand, B. Moore, and J. Stadel, *Mon. Not. Roy. Astron. Soc.* **353**, 624 (2004), astro-ph/0402267.
  - [19] Y. Shikaze et al., *Astropart. Phys.* **28**, 154 (2007), astro-ph/0611388.
  - [20] C. Boehm and P. Fayet, *Nucl. Phys.* **B683**, 219 (2004), hep-ph/0305261.
  - [21] J. Dunkley et al. (WMAP), *Astrophys. J. Suppl.* **180**, 306 (2009), 0803.0586.
  - [22] M. R. Whalley, D. Bourilkov, and R. C. Group (2005), hep-ph/0508110.
  - [23] A. Lewis and S. Bridle, *Phys. Rev.* **D66**, 103511 (2002), astro-ph/0205436.

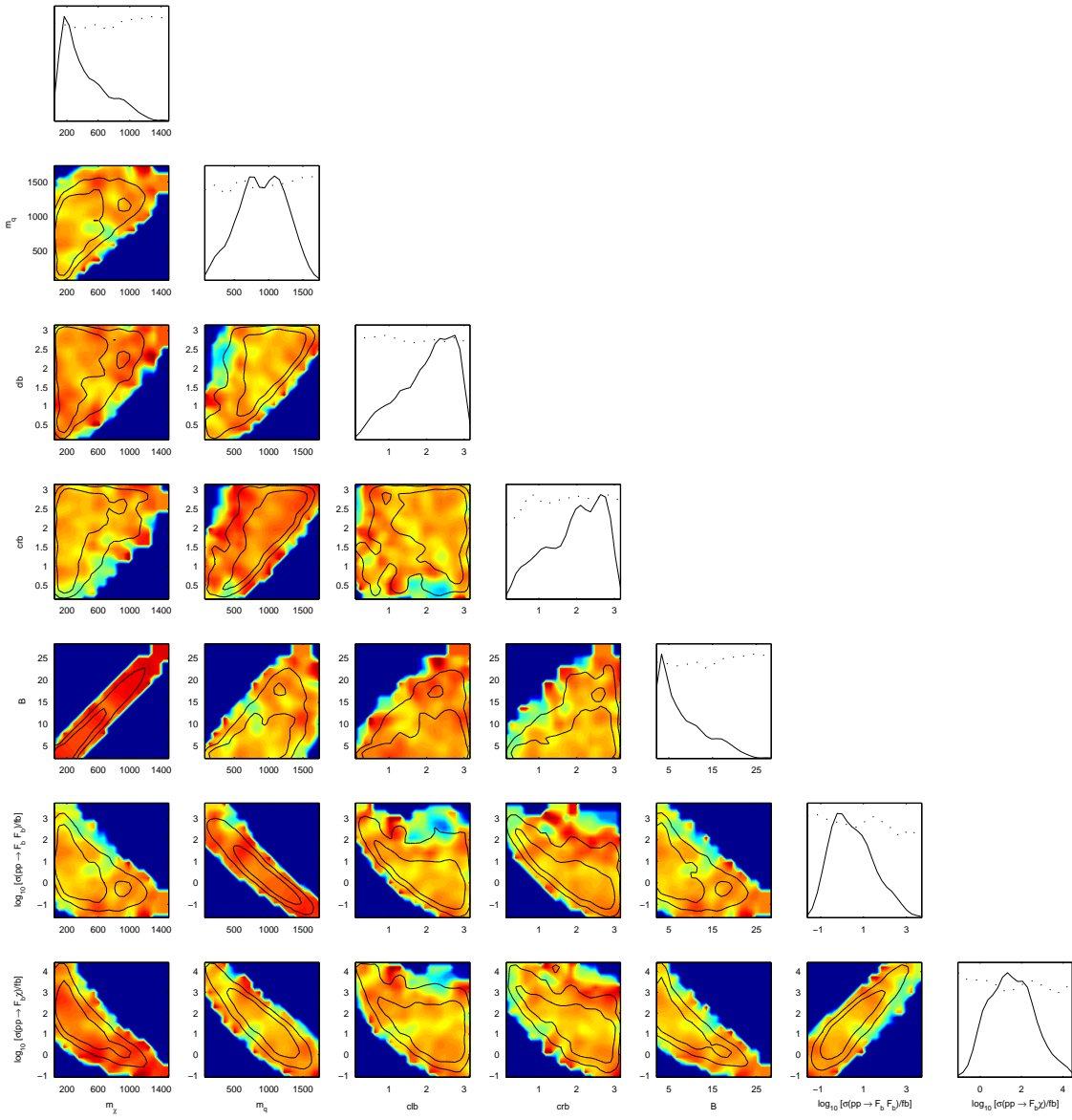


FIG. 3: The dark matter parameter space is tuned to reproduce the boost factor obtained in Sec. II for a  $b\bar{b}$  pair. The central boost value is taken from Tab. I while its variance is estimated from the last five columns of Tab. II. We used the `getdist` routine from the COSMOMC code [23] to make this plot.